

On Attitude Dynamics and Control of Legged Robots Using Tail-Like Systems

Konstantinos Machairas and Evangelos Papadopoulos

School of Mechanical Engineering
National Technical University of Athens
9 Heroon Polytechniou Str., 15780 Athens, Greece
[kmach, egpapado]@central.ntua.gr

ABSTRACT

In this work we study the attitude dynamics and the control of legged robots using tail-like appendages during the aerial phases of high speed locomotion. A free floating two-body system is used to describe the dynamics of a large body controlling its attitude using a rotating appendage. The equations of motion for a tail and a reaction wheel are given, and the meaning of the generalized coordinates being ignorable or palpable is discussed in detail. A thorough discussion on the holonomy of the system is also included. Analytical expressions are given for a further reduced dynamical model and model-based controllers are then proposed. Finally, we present a series of simulation results, and we derive conclusions that can serve as guidelines when designing such systems.

Keywords: Legged Robot, Tail, Reaction Wheel, Attitude Control, Nonholonomic.

1 INTRODUCTION

Over the last five years, research in legged robotics has drawn again the attention of the robotics research community, as universities and companies came up with impressive accomplishments, especially in the field of quadrupedal locomotion. Although much research has been conducted concerning the design and control of legs of various morphologies, attitude control of the body is yet poorly investigated. However, most of the tasks assigned to legged robots, such as high speed galloping or jumping over obstacles, require precise control of the robot's attitude. So far, attitude control is mostly achieved indirectly through the motion of the legs, a technique that assigns more tasks to the legs forcing them to trade-offs that may lead to low performance.

To better mitigate this challenge, dedicated appendages with greater moment of inertia (MoI) can be used. Interesting ideas can be derived from biology; one quickly thinks of animal tails. Many quadruped mammals have long tails, which aid to balance and maneuver at high speeds, [1]. Kangaroo rats use their long tails for righting and turning in midair. Black rats can impressively enter a building by balancing along a 2mm wire. Moreover, studying hopping by kangaroos, one may be amazed to see how they use their tails to counteract the body pitching induced by the motion of their legs, [2]. In general, legged animals mostly use their tails for fine adjustments to perturbations, when their legs are otherwise occupied.

While numerous legged robots have been designed, only a minority employ dedicated appendages for angular momentum management, such as tails or reaction wheels, [3-7]. A number of studies have also dealt with attitude control under conservation of angular momentum, and methods that can lead a mechanism from an initial configuration to a desired final one have been developed, [8-10]. However, to the authors' knowledge, no methodology has been proposed concerning the design of such tail-like mechanisms.

In this work, we use a free floating two-body system to describe the dynamics of a large body controlling its attitude using a rotating appendage. The equations of motion are next given for all cases, and the meaning of the ignorable and palpable coordinates is discussed in detail. To this end, we also clarify several issues concerning the holonomy of the system and its implications on attitude control. The model is then further reduced and model-based controllers

are proposed. Finally, we present a series of simulation results, and we derive conclusions that can serve as guidelines when designing such systems.

2 DYNAMICS AND ANGULAR MOMENTUM

2.1 Dynamics

We introduce a simple planar template of two coupled bodies, i.e. a body and a tail in aerial phase (see Table 1). By body we mean the body with the four legs and the head of a legged robot, except for the tail. This is a reasonable assumption if one considers zero leg MoI and a rigid spine. The uniform gravitational field allows separation of the system center of mass (CoM) motion and the relative motion into two decoupled pieces. Therefore we can decouple the system CoM motion, and obtain a reduction to the system CoM frame. We parameterize the configuration space only by the absolute pitch angle of the body $\theta \in S^1$, and the relative hinge angle of the tail $q \in S^1$. Let (m_0, I_0) and (m_1, I_1) denote the mass and the MoI about each body CoM, for the body and the tail respectively. Let r be the distance from the body CoM to the joint, and l be the distance from the tail CoM to the joint. Finally, let τ be the control torque that the body exerts on the tail, with the motor modelled as an ideal torque source.

The equations of motion (EoM) are given in Table 1 for every possible case, including both reaction wheel and tail cases, with a reaction wheel being any symmetrical body hinged at its own CoM. We note that the two masses appear only in the form of an important quantity $\mu = (m_1 m_2) / (m_1 + m_2)$, that we call the *system effective mass*. In all cases, the generalized coordinates are characterized as *ignorable* or *palpable*, since this distinction can help the analysis. A coordinate is called ignorable or cyclic when it does not appear in the Lagrangian, and palpable or positional otherwise. In practice, when a coordinate is ignorable, we can write the EoM without this coordinate. We note that when the hinge is transferred to the body CoM, the shape angle q turns from palpable to ignorable, with important implications on the system's holonomy, which are discussed next thoroughly.

2.2 Conservation of Angular Momentum

We note that the generalized momentum associated with the ignorable coordinate θ is conserved ($\partial L / \partial \dot{\theta} = \text{const}$, where L is the Lagrangian), yielding:

$$(I_0 + \mu r^2 + I_1 + \mu l^2 + 2\mu r l \cos q) \dot{\theta} + (I_1 + \mu l^2 + \mu r l \cos q) \dot{q} = h_0 \quad (1)$$

which is in fact the equation for the conservation of the system's angular momentum about its CoM, with h_0 being the system initial angular momentum.

2.3 Integrability of the Constraint and System's Holonomy

As thoroughly discussed in [11], the general case of a planar free-floating open kinematic chain is nonholonomic for $n > 2$ bodies. However, in literature, the two-body system is often incorrectly considered either holonomic or nonholonomic without the appropriate analysis. In this work, the problem is addressed in detail, and it is shown that the system's holonomy depends on the system's geometry and the system's initial angular momentum.

Equation (1) can take the form of an acatastatic Pfaffian constraint, which is nonholonomic only when $r, l \neq 0$ and $h_0 \neq 0$ at the same time. This means that for zero initial angular momentum, the conservation equation is analytically integrable independent of the position of the hinge. When time enters as a third variable through the initial angular momentum, the constraint is integrable only if the tail is pinned at the body CoM ($r=0$), or if the appendage is a reaction wheel. A holonomic constraint is in fact a geometric one and thus each θ corresponds to a specific q , while a nonholonomic constraint makes the whole configuration manifold accessible,

Table 1. EoM for systems of different geometries.

	<p>General case: 2-body free floating system θ: ignorable, q: palpable</p> $(I_0 + \mu r^2 + I_1 + \mu l^2 + 2\mu r l \cos q)\ddot{\theta} + (I_1 + \mu l^2 + \mu r l \cos q)\ddot{q} - \mu r l \sin q(\dot{q}^2 + 2\dot{q}\dot{\theta}) = 0 \quad (2)$ $(I_1 + \mu l^2 + \mu r l \cos q)\ddot{\theta} + (I_1 + \mu l^2)\ddot{q} + \mu r l \sin q\dot{\theta}^2 = \tau$
	<p>Tail hinged at distance r from body CoM ($I_1=0$) θ: ignorable, q: palpable</p> $(I_0 + \mu r^2 + \mu l^2 + 2\mu r l \cos q)\ddot{\theta} + (\mu l^2 + \mu r l \cos q)\ddot{q} - \mu r l \sin q(\dot{q}^2 + 2\dot{q}\dot{\theta}) = 0 \quad (3)$ $(\mu l^2 + \mu r l \cos q)\ddot{\theta} + \mu l^2\ddot{q} + \mu r l \sin q\dot{\theta}^2 = \tau$
	<p>Tail hinged at body CoM ($I_1=0, r=0$) θ: ignorable, q: ignorable</p> $I_0\ddot{\theta} = -\tau$ $\frac{I_0\mu l^2}{I_0 + \mu l^2}\ddot{q} = \tau \quad (4)$
	<p>Reaction wheel hinged at distance r from body CoM ($l=0$) θ: ignorable, q: ignorable</p> $(I_0 + \mu r^2)\ddot{\theta} = -\tau$ $\frac{I_1(I_0 + \mu r^2)}{I_0 + I_1 + \mu r^2}\ddot{q} = \tau \quad (5)$
	<p>Reaction wheel hinged at body CoM - "Elroy's Beanie", [12], ($l=r=0$) θ: ignorable, q: ignorable</p> $I_0\ddot{\theta} = -\tau$ $\frac{I_1 I_0}{I_0 + I_1}\ddot{q} = \tau \quad (6)$

and any pair (θ, q) can be achieved. Next, we present the holonomic cases, and we give analytical results based on the analysis in [13].

Zero Initial Angular Momentum

In this case, the conservation equation is integrable for all geometries. Integrating (1) with $h_0=0$ yields:

$$\theta = \theta_0 - \frac{1}{2}(q - q_0) - \frac{A}{C} \tan^{-1}\left(\frac{B}{C} \tan \frac{q}{2}\right) + \frac{A}{C} \tan^{-1}\left(\frac{B}{C} \tan \frac{q_0}{2}\right) \quad (7)$$

where

$$A=I_1+\mu l^2-I_0-\mu r^2, B=I_0+I_1+\mu(l-r)^2$$

$$C=\sqrt{(I_0+I_1+\mu l^2+\mu r^2)^2-(2\mu rl)^2}$$

This is a rather involved expression that gets much simpler when $r=0$ (the appendage is hinged at the body's CoM), or $l=0$ (the appendage rotates about its CoM, i.e. it is a reaction wheel).

Nonzero Initial Angular Momentum

For nonzero angular momentum, the more general case in which (1) is integrable is when the appendage is hinged at body CoM. Integrating (1) with $r=0$ yields:

$$(I_0+I_1+\mu l^2)(\theta-\theta_0)+(I_1+\mu l^2)(q-q_0)=h_0(t-t_0) \quad (8)$$

Conclusions

- When both generalized coordinates are ignorable, the conservation equation is always integrable and the system holonomic.
- When both coordinates are ignorable, the inertia matrix becomes independent of the shape variable q , the EoM can be written decoupled, and analytical solutions can be derived.
- When the initial angular momentum is zero, the system is holonomic for every geometry. Hence, it is not possible to achieve any pair of θ and q .
- When the appendage is a reaction wheel, the system is always holonomic.
- The system is nonholonomic only when a tail ($l \neq 0$) is hinged at a distance $r \neq 0$ from the body CoM and the initial angular momentum is nonzero.

3 REDUCED DYNAMICS AND CONTROL

Being difficult to control both θ and q with a single control input τ , we develop model-based controllers to control θ when we need to control the body attitude, and q when we need to position the tail to a desired angle.

3.1 Control of the Tail Angle q

For all cases θ is an ignorable coordinate; we can derive the reduced EoM in the form of a single equation where only q , \dot{q} and \ddot{q} appear (see Appendix for the full expressions):

$$D(q)\ddot{q}+C(q,\dot{q})\dot{q}+G(q,h_0^2)=\tau \quad (9)$$

Using (9) the following feedback linearization control scheme can be applied in order to control the tail angle q , where e_q is the error in tail angle, and k_v , k_p are the gains of a PD controller:

$$\tau=D(q)(\ddot{q}_d+k_v\dot{e}_q+k_p e_q)+C(q,\dot{q})\dot{q}+G(q,h_0^2) \quad (10)$$

3.2 Control of the Unactuated Body Angle θ

In order to control θ one should eliminate \ddot{q} from the second EoM (1), yielding a single equation of the form (see Appendix for the full expressions):

$$D^*(q)\ddot{\theta}+C^*(q,\dot{q},\dot{\theta})=\tau \quad (11)$$

Similarly to the previous case, a model-based controller is developed for θ , achieving $\ddot{\theta}=\ddot{\theta}_{des}$:

$$\tau=D^*(q)(\ddot{\theta}_d+k_v\dot{e}_\theta+k_p e_\theta)+C^*(q,\dot{q},\dot{\theta}) \quad (12)$$

Trajectory planning is implemented using a quintic polynomial of the following form (see Appendix for the full expressions):

$$\theta_{des}(t) = a_0 + a_1t + a_2t^2 + a_3t^3 + a_4t^4 + a_5t^5 \quad (13)$$

The control scheme described here was used in all the experiments included in this work.

4 DESIGN PRINCIPLES

The analysis above is important for the attitude control of a legged robot, and provides the basic guidelines for building a design methodology for tail-like systems. On this basis, steps for selection of the key parameters of reaction wheels and tails have been proposed in [13]. In this section we focus on tail design, since a tail has been proved to be more effective than a wheel, [13]. The main parameters to be selected are the mass and the length of the tail, while the motor characteristics are also of great importance. Depending on the case, several criteria can be used for the calculation of these parameters. These concern: (a) the maximum change of the body angle that can be achieved during a flight phase, (b) the maximum body angular velocity that can be rejected through the tail's motion, (c) the maximum accelerating or decelerating force appearing at the tail joint, and (d) the maximum change on body's angular momentum induced by leg motion. The design principles introduced herein are mainly based on the first criterion.

Suppose the body needs to perform a maneuver $\Delta\theta$ in a specific time interval Δt in roll, pitch or yaw direction. In this case, a suitable torque profile $\tau(t)$ must be provided by the tail-like appendage to rotate the body. The device can only deliver the torque needed, if a motor can accelerate the appendage by exerting on it the opposite torque. As expected, when the desired torque is exerted on a low MoI appendage, high angular acceleration and thus high angular velocity results, and this greatly affects the characteristics that the motor should have. For instance, a demanding task requires the motor to work in high torque (in order to rotate the body), and high speed (the speed that the lower MoI appendage reaches). Besides, the appendage's mass must be the lowest possible, so that a robot can use it without significantly increasing its total mass. These facts reveal the importance of the proper appendage design, and how this affects the selection of the driving motor.

In most cases, the rotation of the tail is mechanically constrained, as also observed in animal tails, and thus every maneuver must be completed while the appendage is within its mechanical bounds, i.e. $q \in [q_{min}, q_{max}]$. Considering the conservation equation in the zero initial angular momentum case, when Δq is bounded, $\Delta\theta$ is also bounded, i.e. not every desired maneuver can be performed. Hence, the parameters consisting this equation are significant for a proper design and determine the capabilities of the final device. On this basis, an expression for the tail mass calculation has been proposed in [13], which is also used in this work. At this point, we reach the following conclusions that we will validate through simulation experiments in section 5:

- *By choosing the tail mass after maximizing the tail length, one chooses the maximum body maneuver $\Delta\theta$ that can be performed when the system total angular momentum is zero, or the maximum initial body angular velocity that can be rejected in a time interval Δt , when the system initial angular momentum is nonzero.*
- *The time interval to complete a maneuver is determined by the torque provided by the tail; the higher the torque, the faster the maneuver. Moreover, the lower the tail mass, the higher the tail acceleration under a certain torque profile, and therefore, the greater the power needed.*

5 SIMULATION EXPERIMENTS

In our previous work, we have shown that a tail hinged at distance r from the body CoM is a better solution than a reaction wheel hinged at the same position; since the required motor power, and torque are significantly reduced in the tail case, [13]. Therefore, in this section, we present a series of simulation experiments of bodies performing maneuvers with tails of various

morphologies, to better understand the nature of the problem. Zero initial angular momentum was considered in all experiments, in order to reach conclusions easier. We were mostly interested in the control torque profile, and the maximum tail angular speed since, these are the parameters that mainly determine the motor selection. Considering DC actuators, the selection of a motor-gearbox-amplifier combination that can perform such maneuvers, is difficult or sometimes impossible. The speed – torque characteristics for a demanding maneuver often exceed the capabilities of typical DC actuators, and even if there is a suitable actuator for the task, its mass can be unacceptable. These difficulties lie mainly on the need to control the attitude of a large MoI body by rotating a small MoI appendage in a very short time interval. These facts make the following analysis valuable, since the limits regarding the actuators and the possible maneuvers are revealed through numerous experiments. The parameters of the simulations were chosen according to data obtained from animal and robot locomotion, [13].

5.1 Experiments varying the Tail Mass

First, we consider a body of mass $m_0=30\text{kg}$ and MoI $I_0=2\text{kgm}^2$, performing a $\Delta\theta=3^\circ$ maneuver in 0.15s using a tail hinged at distance $r=0.4\text{m}$ from the body CoM, with tail length $l=0.4\text{m}$, tail mass varying from 0.5 to 4 kg, and $I_1=0$. We use the expression given in [13] to calculate a minimum value for the tail mass, and with this in mind, we try greater values to see how other parameters, such as motor torque, speed, and power change. This is the first experiment, since the mass of the tail is the easiest parameter to change in a real robot. Simulation results are shown in Fig. 1.

Conclusions

In Figures 1(c) and 1(d), we see that for greater tail mass the maximum motor speed decreases, while the maximum torque slightly increases. Furthermore, the power that the motor has to deliver is much greater for lower tail mass, see Fig. 1(f). We conclude that the greater the tail mass, the better for the actuator, provided that the maximum torque can be supplied by the actuator, and the extra mass can be carried by the robot. Therefore, a good choice for the tail mass would be $m_1=1.5\text{kg}$, and thus this is the value used in the following experiments.

5.2 Experiments varying the Tail Length

Except for changing the tail mass, another way to change the tail MoI about its hinge is by changing the tail length l . In this series of simulations, we use the same parameters as above, with a tail mass of 1.5kg, and a tail length varying from 0.2m to 0.5m, to achieve a $\Delta\theta=3^\circ$ maneuver in 0.15s. Simulation results are shown in Fig. 2.

Conclusions

We reach similar conclusions with the previous case, in which we varied the tail mass, i.e. the greater the tail mass, the better for the actuator, provided that the maximum torque can be supplied, see Fig. 2(e). However, in this case, a limit exists for the tail length mostly due to the robot's geometry. For instance, it cannot be much greater than the leg's length.

5.3 Experiments varying the Body CoM – Hinge Distance

In this section we present simulation results from experiments of a $\Delta\theta=10^\circ$ maneuver in $\Delta t=0.2\text{s}$, and different hinge positions, varying the body CoM – hinge distance r from 0m to 0.45m. The rest of the parameters are kept similar to the ones in the previous simulations. The results are shown in Fig. 3.

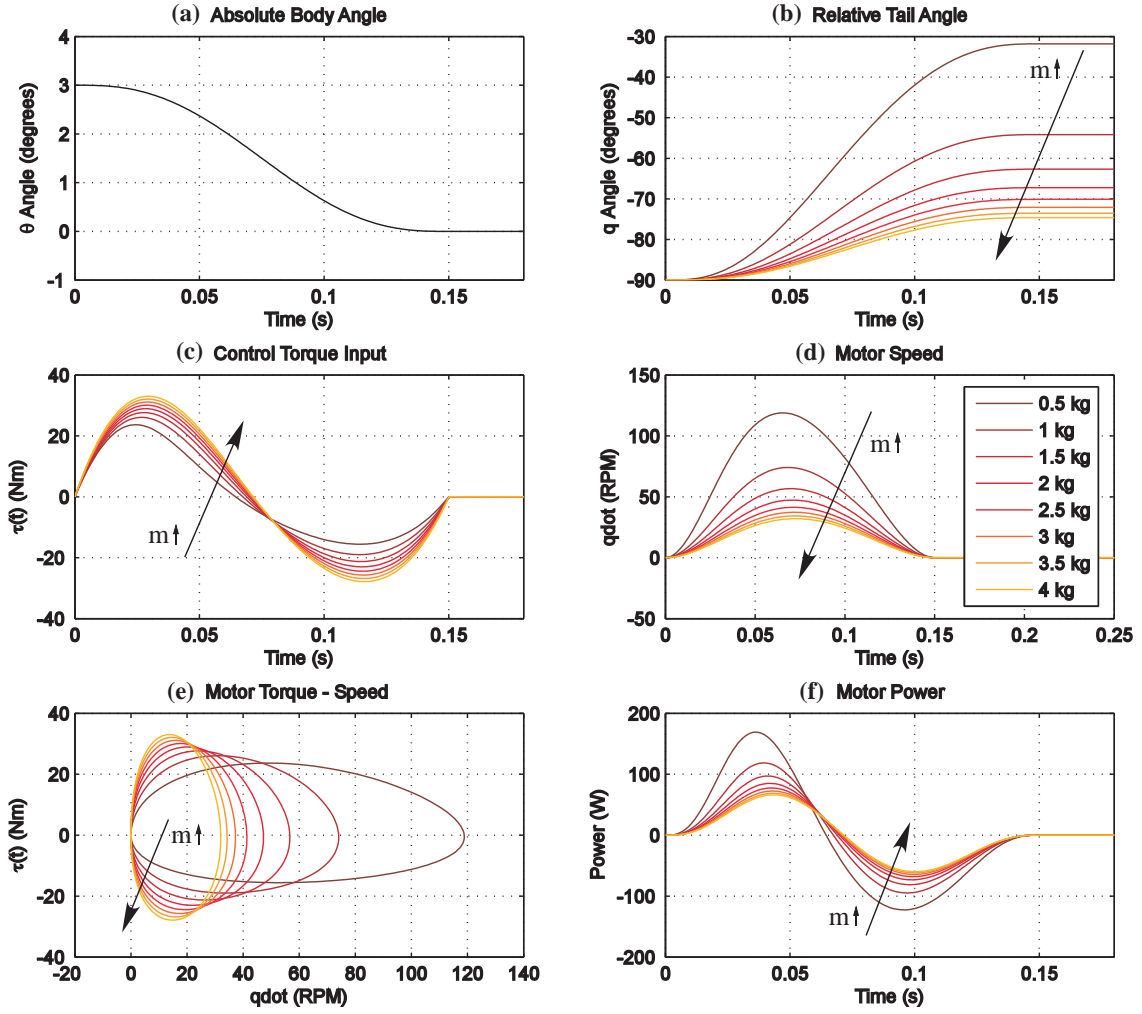


Figure 1. A body of $m_0=30\text{kg}$, $I_0=2\text{kgm}^2$, with a tail of length $l=0.4\text{m}$, MoI $I_1=0$, and mass m_1 varying from 0.5kg to 4kg , hinged at distance $r=0.4\text{m}$ from the body CoM, performs a maneuver of $\Delta\theta=3^\circ$ in $\Delta t=0.15\text{s}$.

Conclusions

As shown in Figures 3(c), 3(d), and 3(f), the torque, speed and power profiles are symmetric when the tail is hinged at the body CoM. In every other case, where $r \neq 0$, the hinge force creates a torque that breaks this symmetry and helps the motor perform the maneuver. As a result, the motor torque, speed and power decrease as the body CoM – hinge distance increases, i.e. the greater this distance is, the easier for the actuator to perform a certain maneuver.

5.4 Experiments varying the Time of the Maneuver

It is evident so far that the time interval chosen for a certain maneuver is a key parameter of the task, and strongly affects the motor selection. In this series of simulations we address this topic systematically by performing a $\Delta\theta = 10^\circ$ maneuver in different time intervals Δt , varying from 0.15s to 0.4s . The body and tail parameters are: $m_0=30\text{kg}$, $m_1=1.5\text{kg}$, $I_0=2\text{kgm}^2$, $I_1=0$, $l=0.4\text{m}$, and $r=0.4\text{m}$. The results are presented in Fig. 4.

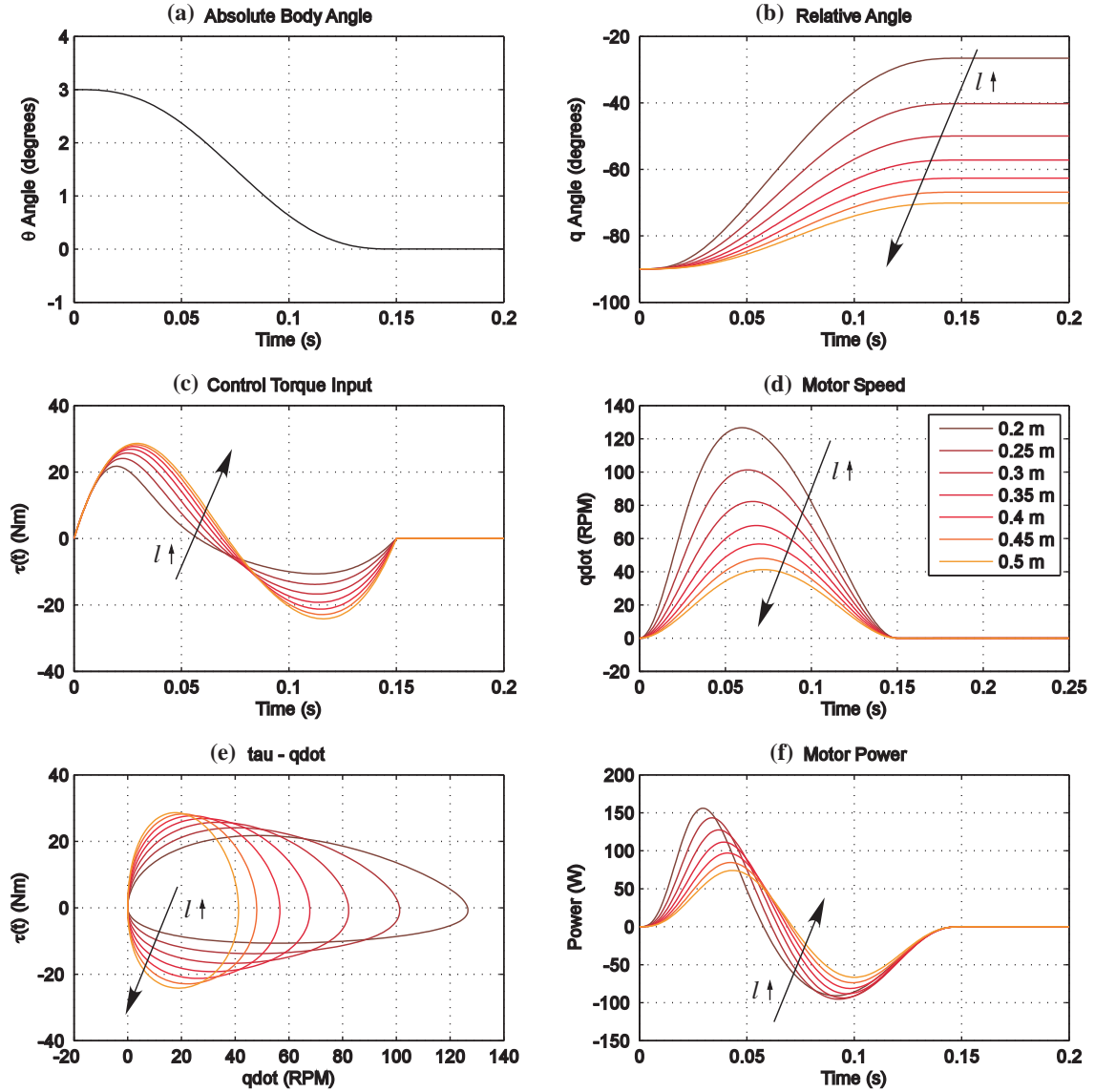


Figure 2. A body of $m_0=30\text{kg}$, $I_0=2\text{kgm}^2$, with a tail of mass $m_1=1.5\text{kg}$, MoI $I_1=0$, and length l varying from 0.2m to 0.5m , hinged at distance $r=0.4\text{m}$ from the body CoM, performs a maneuver of $\Delta\theta=3^\circ$ in $\Delta t=0.15\text{s}$.

Conclusions

Figures 4(c), 4(d), and 4(f) show that by decreasing the time available for the maneuver, the motor power, torque and speed increase. The very short time interval is the main reason for the need of powerful motors that would be of no use for longer time intervals. The torque and power requirements decrease significantly even for a desired time of 0.4s . Moreover, the tail angle – time diagram reveals the time invariance of the holonomic angular momentum constraint (note that the initial angular momentum is zero in this experiment), since the change in tail angle is the same for all experiments, see Fig. 4(b).

5.5 Experiments varying the Body MoI

Legged robots are systems that must be able to move successfully with varying inertia properties. Two typical reasons are the need to carry different cargos, and the uncertainty regarding the knowledge of the robot's real inertia properties. This fact justifies the analysis presented in the section, which includes simulation experiments with bodies of different MoI controlling their attitude with identical tails. Maneuvers of $\Delta\theta=3^\circ$ in $\Delta t=0.15\text{s}$ are performed by

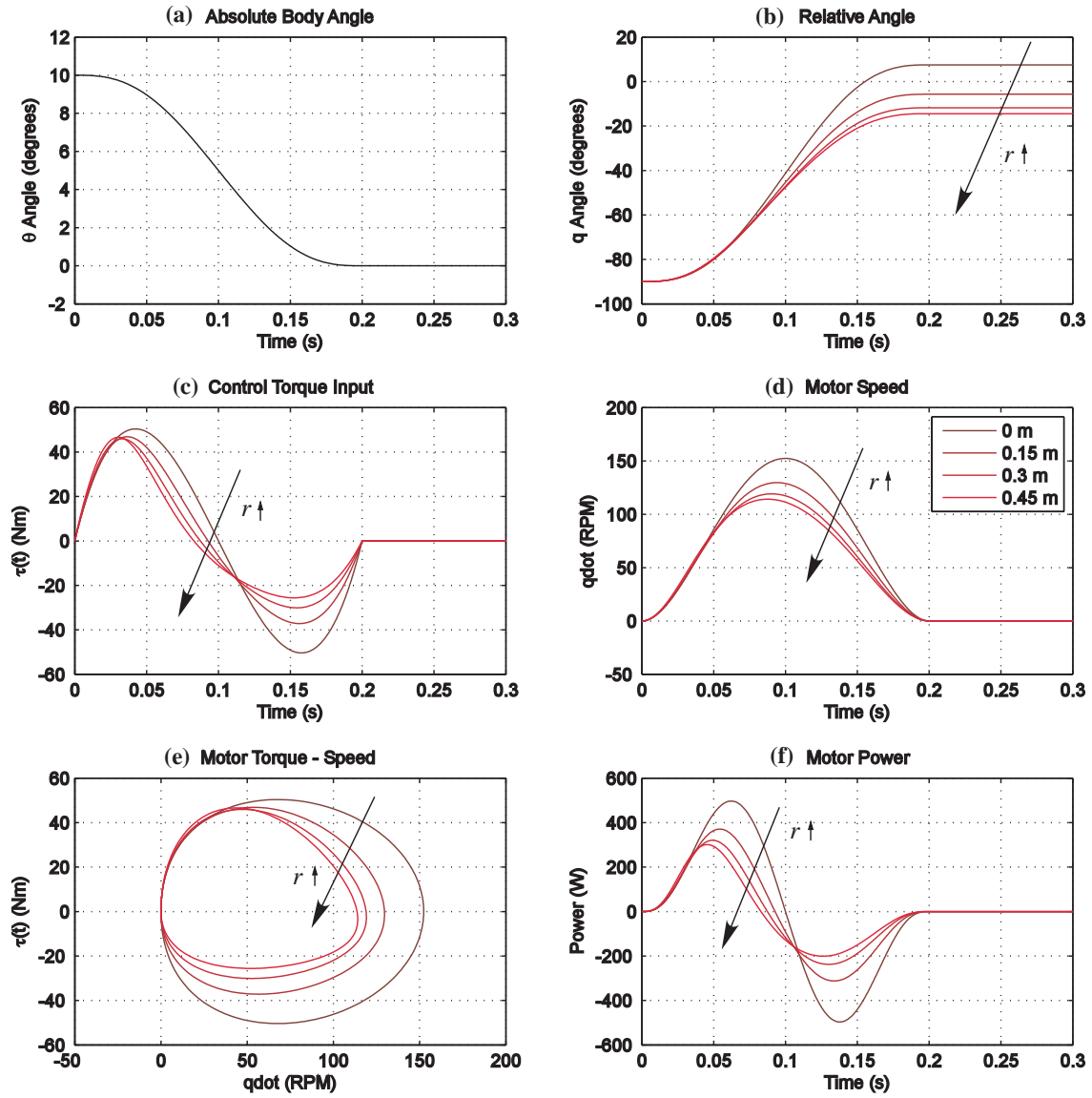


Figure 3. A body of $m_0=30\text{kg}$, $I_0=2\text{kgm}^2$, with a tail of mass $m_1=1.5\text{kg}$, MoI $I_1=0$, and length $l=0.4\text{m}$, hinged at a distance r from body CoM, which varies from 0m to 0.45m, performs a maneuver $\Delta\theta=10^\circ$ in $\Delta t=0.2\text{s}$.

bodies of MoI from 1.6 to 2.4 kgm^2 . The other simulation parameters are: $m_0=30\text{kg}$, $m_1=1.5\text{kg}$, $I_1=0$, $l=0.4\text{m}$, and $r=0.4\text{m}$. The results are shown in Fig. 5.

Conclusions

As expected, for bodies of greater MoI, greater power, torque and speed are requested from the motor, see Figures 5(c), 5(d), and 5(f). Hence, the greater the body MoI, the harder for the actuator to perform a certain maneuver, see Fig. 5(e).

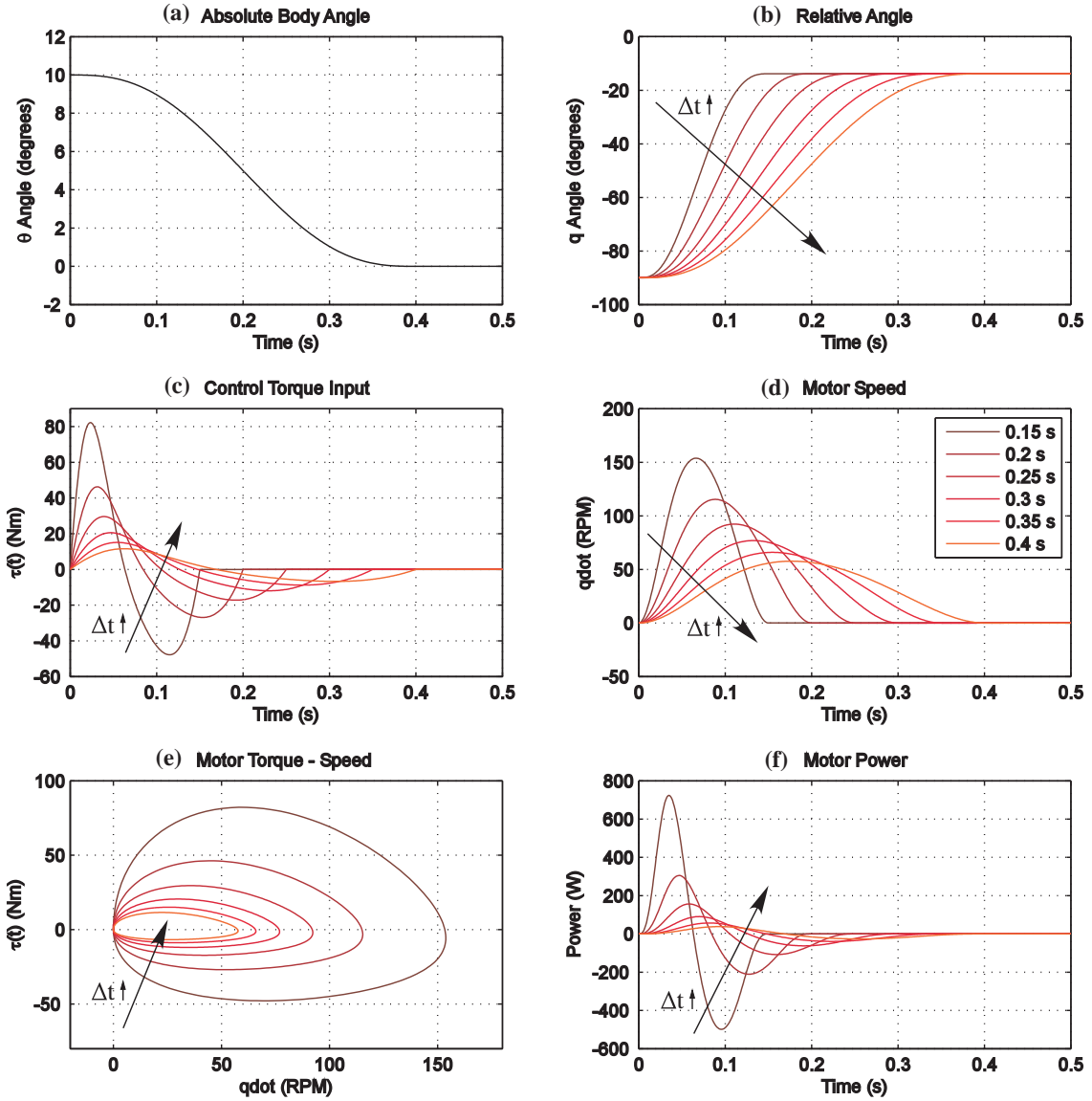


Figure 4. A body of $m_0=30\text{kg}$, $I_0=2\text{kgm}^2$, with a tail of mass $m_1=1.5\text{kg}$, MoI $I_1=0$, and length $l=0.4\text{m}$, hinged at a distance $r=0.4\text{m}$ from the body CoM, performs a $\Delta\theta=10^\circ$ maneuver in time intervals Δt varying from 0.15 to 0.4s.

6 CONCLUSIONS

In this paper we studied the attitude dynamics and the control of legged robots using tail-like appendages during the aerial phases of high speed locomotion. A free floating two-body system was introduced to describe the dynamics of a large body controlling its attitude using a rotating appendage. The equations of motion for a tail and a reaction wheel were given, and the meaning of the ignorable and palpable coordinates of the system was discussed in detail. The holonomy of the system was also discussed thoroughly. Analytical expressions were given for a further reduced dynamical model and model-based controllers were proposed. A series of simulation experiments were finally carried out for various system parameters, and important conclusions were derived concerning the design of such systems.

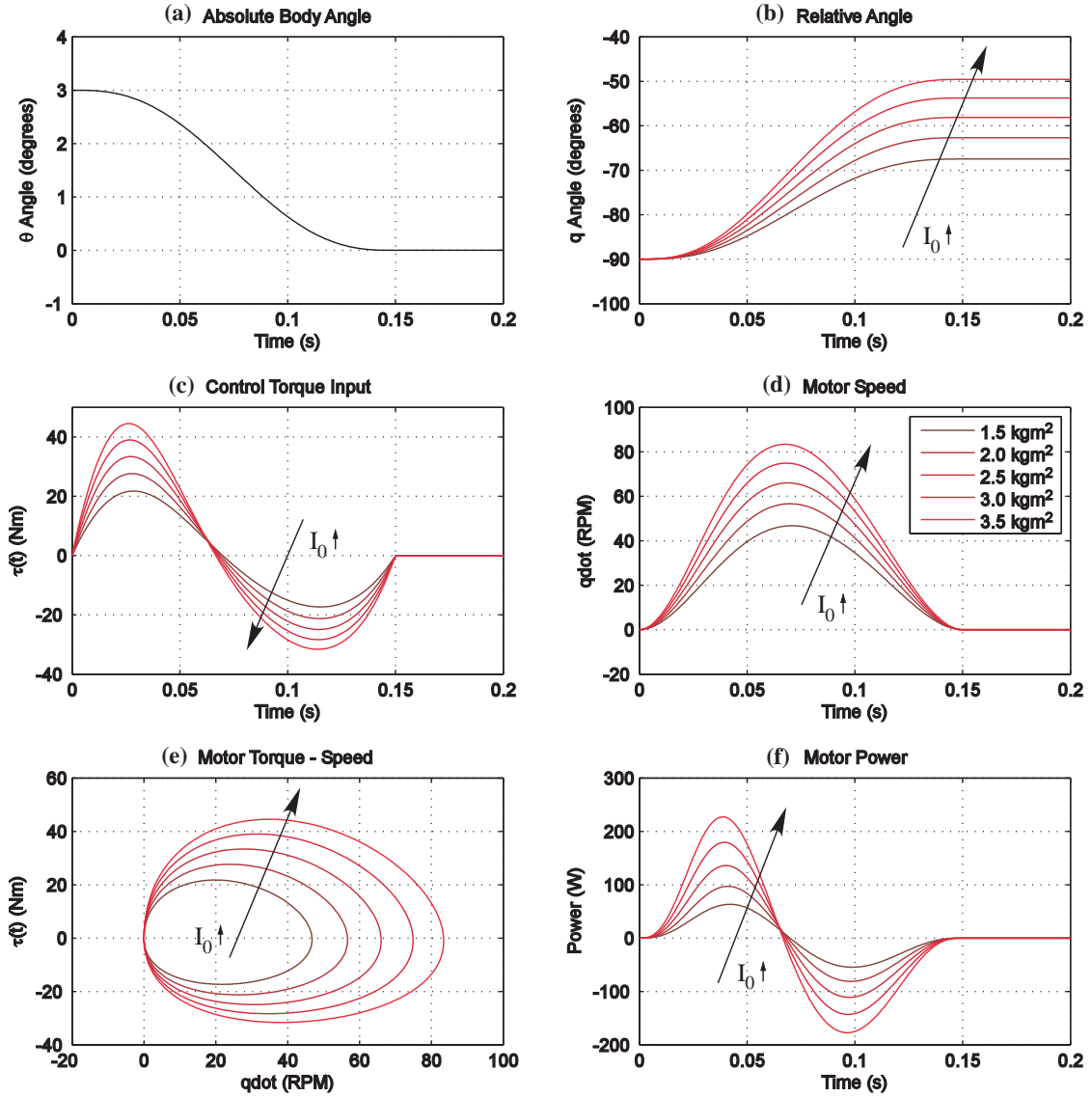


Figure 5. A body of $m_0=30\text{kg}$, and MoI I_0 varying from 1.5 to 3.5kgm^2 , with a tail of length $l=0.4\text{m}$, MoI $I_1=0$, and mass $m_1=1.5\text{kg}$ hinged at $r=0.4\text{m}$ from body CoM performs a $\Delta\theta=3^\circ$ maneuver in $\Delta t=0.15\text{s}$.

ACKNOWLEDGMENT

This research has been financed by the European Union (European Social Fund – ESF) and Greek national funds through the Operational Program “Education and Lifelong Learning” of the National Strategic Reference Framework (NSRF) – Research Funding Program: ARISTEIA: Reinforcement of the interdisciplinary and/ or inter-institutional research and innovation.

REFERENCES

- [1] Hickman, G. C., “The mammalian tail: a review of functions,” *Mammal Review*, 9:143–157, 1979.
- [2] Alexander, R. McN. and Vernon, A., “The mechanics of hopping by kangaroos (Macropodidae),” *Journal of Zoology*, 177: 265-303, 1975.
- [3] De, A., and Koditschek, D. E. (2015). The Penn Jerboa: A Platform for Exploring Parallel Composition of Templates. *arXiv preprint arXiv:1502.05347*.
- [4] Briggs, Randall, et al., “Tails in biomimetic design: Analysis, simulation, and experiment,” (*IROS*), *IEEE/RSJ Int. Conf. on Intelligent Robots and Systems*, 2012.

- [5] <http://spectrum.ieee.org/automaton/robotics/robotics-hardware/fast-running-biped-robot-based-on-velociraptor>
- [6] Johnson, Aaron M., et al. "Tail assisted dynamic self-righting," *Proceedings of the Fifteenth Int. Conf. on Climbing and Walking Robots and the Support Technologies for Mobile Machines*, Baltimore, MD, USA, July 2012.
- [7] Kohut, N. J., et al. "Precise dynamic turning of a 10 cm legged robot on a low friction surface using a tail," *(ICRA), 2013 IEEE Int. Conf. on Robotics and Automation*, 2013.
- [8] Papadopoulos, E., Fragkos, I., & Tortopidis, I., "On robot gymnastics planning with non-zero angular momentum," *IEEE Int. Conf. on Robotics and Automation*, 2007.
- [9] Xin, X., Mita, T., & Kaneda, M., "The posture control of a two-link free flying acrobat with initial angular momentum," *IEEE Transactions on Automatic Control* 49.7: 1201-1206, 2004.
- [10] Sadati, Nasser, et al., "Hybrid Control and Motion Planning of Dynamical Legged Locomotion," Vol. 2. John Wiley & Sons, 2012.
- [11] De Luca, A., & Oriolo, G. (1995). Modelling and control of nonholonomic mechanical systems (pp. 277-342). Springer Vienna.
- [12] Bloch, A. M., Nonholonomic mechanics and control (Vol. 24). Springer Science & Business Media, 2003.
- [13] Machairas, K. and Papadopoulos, E., "On Quadruped Attitude Dynamics and Control Using Reaction Wheels and Tails," *Proc. of the European Control Conference 2015*, Johannes Kepler University, Linz, Austria, July 15-17, 2015.

APPENDIX

Terms of the reduced EoM (9), when written as functions of q, \dot{q}, \ddot{q} :

$$\begin{aligned}
 D(q) &= (d_{00}d_{11} - d_{10}^2) / (d_{00} + d_{11} + 2d_{10}) \\
 C(q, \dot{q}) &= (d_{00} + d_{10})(d_{11} + d_{10})\hat{d}_{10}\dot{q} / (d_{00} + d_{11} + 2d_{10})^2 \\
 G(q, h_0^2) &= \hat{d}_{10}h_0^2 / (d_{00} + d_{11} + 2d_{10})^2 \\
 d_{00} &= I_0 + \mu r^2, \quad d_{11} = I_1 + \mu l^2, \quad d_{10} = \mu r l \cos q, \quad \hat{d}_{10} = \mu r l \sin q
 \end{aligned}$$

Terms of the reduced EoM (11), when written as functions of $q, \dot{\theta}, \ddot{\theta}$:

$$\begin{aligned}
 D^*(q) &= -\frac{d_{11}(d_{00} + d_{11} + 2d_{10})}{d_{11} + d_{10}} + d_{11} + d_{10} \\
 C^*(q, \dot{q}, \dot{\theta}) &= \frac{d_{11}\hat{d}_{10}(\dot{q}^2 + 2\dot{q}\dot{\theta})}{d_{11} + d_{10}} + \hat{d}_{10}\dot{\theta}^2 \\
 &\text{With } d_{00}, d_{11}, d_{10} \text{ and } \hat{d}_{10} \text{ defined above}
 \end{aligned}$$

Terms of the quintic polynomial used for trajectory planning in (13):

$$\begin{aligned}
 a_0 &= \theta_0, \quad a_1 = \dot{\theta}_0, \quad a_2 = \frac{1}{2}\ddot{\theta}_0 \\
 a_3 &= \frac{1}{2t_f^3} (20(\theta_f - \theta_0) - (8\dot{\theta}_f + 12\dot{\theta}_0)t_f - (3\ddot{\theta}_0 - \ddot{\theta}_0)t_f^2) \\
 a_4 &= \frac{1}{2t_f^4} (-30(\theta_f - \theta_0) + (14\dot{\theta}_f + 16\dot{\theta}_0)t_f + (3\ddot{\theta}_0 - 2\ddot{\theta}_0)t_f^2) \\
 a_5 &= \frac{1}{2t_f^5} (12(\theta_f - \theta_0) - 6(\dot{\theta}_f + \dot{\theta}_0)t_f + (\ddot{\theta}_0 - \ddot{\theta}_0)t_f^2)
 \end{aligned}$$